Products and Mechanism of the Reaction of Cl with Butanone in N_2/O_2 Diluent at 297−526 K

E. W. Kaiser,*,†,‡ T. J. Wallington,*,§ and M. D. Hurley§

Department of Natural Sciences, University of Michigan−Dearborn, 4901 Evergreen Road, Dearborn, Michigan 48128, and System Analytics and Environmental Science Department, Research and Innovation Center, Ford Motor Company, Mail Drop RIC-2122, Dearborn, Michigan 48121-2053

Received: October 16, 2008; Revised Manuscript Received: December 26, 2008

The products, kinetics, and mechanism of the reaction Cl + butanone have been measured by UV irradiation of Cl_2/butanone/N_2 (O_2) mixtures using either GC or FTIR analysis. In the absence of O_2, the products are 1-, 3-, and 4-chlorobutanone with yields of 3.1%, 76%, and 22.5%, respectively. As the temperature is increased, the yields of 1- and 4-chlorobutanone increase relative to the 3-chlorobutanone yield. On the basis of these increases, the activation energies for hydrogen abstraction at the 1 and 4 positions are determined to be 1800 (±300) and 470 (+300, −150) cal mol^{-1} relative to abstraction at the 3 position. In the presence of 400 ppm of O_2 with 700−900 ppm of Cl_2 at 297 K, the yields of 1- and 3-chlorobutanone decrease dramatically from 3.1% to 0.25% and from 76% to 2%, respectively, while the 4-chlorobutanone decreases only slightly from 22.5% to 18.5%. The observed oxygenated species are acetaldehyde (52%), butanedione (11%), and propionyl chloride (2.5%). Increasing the temperature to 400 K (O_2 = 500 ppm) suppresses these oxygenated products and 1- and 3-chlorobutanone again become the primary products, indicating that the O_2 addition reaction to the 1- and 3-butanonyl radicals is becoming reversible. At 500 K and very high O_2 mole fraction (170 000 ppm), a new product channel opens which forms a substantial yield (∼20%) of methylvinylketone. Computer modeling of the product yields has been performed to gain an understanding of the overall reaction mechanism in the presence and absence of O_2. The reaction of chlorine atoms with butanone proceeds with a rate constant of 4.0 (±0.4) × 10^{-11} cm^3 molecule^{-1} s^{-1} independent of temperature over the range 297−475 K ($E_a = 0 \pm 200$ cal mol^{-1}). Rate constant ratios of $k(CH_2C(O)C_2H_5 + Cl_2)/k(CH_2C(O)C_2H_5 + O_2) = 0.027 \pm 0.008$, $k(CH_3C(O)CHCH_3 + Cl_2)/ k(CH_3C(O)CHCH_3 + O_2) = 0.0113 \pm 0.0011$, and $k(CH_3C(O)CH_2CH_2 + Cl_2)/k(CH_3C(O)CH_2CH_2 + O_2) = 1.52 \pm 0.32$ were determined at 297 K in 800−950 Torr of N_2 diluent. In 700−900 Torr of N_2/O_2 diluent, the major fate of the alkoxy radicals $CH_3C(O)CH(O)CH_3$ and $OCH_2C(O)C_2H_5$ is decomposition to give $CH_3C(O)$ radicals and CH_3CHO and HCHO and $C(O)C_2H_5$ radicals, respectively.

1. Introduction

Recent publications have presented measurements of the rate constant of the reaction of Cl atoms with butanone at ambient temperature (see ref 1 and citations therein). However, data regarding the products of this hydrogen abstraction reaction are very limited. The only mechanistic measurements available to our knowledge were obtained by Iwasaki et al.[2] using UV irradiation of Cl_2/N_2/butanone mixtures. They identified the 3-butanonyl radical ($CH_3C(O)CHCH_3$) as the major abstraction product with a yield of 73 ± 9%, based on the measured yield of 3-chlorobutanone. No other products could be quantified in their FTIR spectroscopy experiments. To improve our understanding of the oxidation mechanism of ketones in general and butanone specifically, we have extended the study of Iwasaki et al.[2] to include a range of temperatures, oxygen partial pressures, and total pressures.

The results presented herein are obtained using primarily GC/FID (gas chromatography with flame ionization detector) and GC/MS (mass spectrometric detector) analysis systems. As in the case of Iwasaki et al., the reaction is studied by UV irradiation of $Cl_2/N_2/O_2$/butanone mixtures. Limited data were also obtained using FTIR spectroscopy. Using the GC method, the yields of most products formed by the Cl reaction both in the presence and absence of O_2 could be measured. This allows a determination of both oxidative and nonoxidative reaction pathways of the butanonyl radicals formed in the three channels of reaction 1:

$$Cl + CH_3C(O)CH_2CH_3 \rightarrow CH_3C(O)CHCH_3 + HCl \quad (1a)$$

$$Cl + CH_3C(O)CH_2CH_3 \rightarrow CH_3C(O)CH_2CH_2 + HCl \quad (1b)$$

$$Cl + CH_3C(O)CH_2CH_3 \rightarrow CH_2C(O)CH_2CH_3 + HCl \quad (1c)$$

In the absence of O_2, the 1-, 3-, and 4-butanonyl radicals react with the Cl_2 present in the unreacted mixture to form 1-, 3-, and 4-chlorobutanones via reaction 2:

$$CH_3C(O)CHCH_3 + Cl_2 \rightarrow CH_3C(O)CHClCH_3 + Cl \quad (2a)$$

$$CH_3C(O)CH_2CH_2 + Cl_2 \rightarrow CH_3C(O)CH_2CH_2Cl + Cl \quad (2b)$$

$$CH_2C(O)CH_2CH_3 + Cl_2 \rightarrow CH_2ClC(O)CH_2CH_3 + Cl \quad (2c)$$

In the presence of O_2, the products observed include acetaldehyde, acetyl chloride, butanedione, propionyl chloride, and

* Corresponding authors. E-mail: ewkaiser@comcast.net (E.W.K.); twalling@ford.com (T.J.W.).
† University of Michigan−Dearborn.
‡ Mailing address: 7 Windham Lane, Dearborn, MI 48120.
§ Ford Motor Company.

10.1021/jp809169h CCC: $40.75
Published on Web 02/19/2009

methylvinylketone (MVK). The reaction channels both in the presence and absence of O_2 have also been studied as a function of temperature (297−526 K), and in limited tests as a function of total pressure. The results of these experiments provide important kinetic and mechanistic insight into the reactions of butanone and butanonyl radicals.

2. Experimental Section

At ambient temperature, a spherical (500 cm^3), Pyrex reactor was employed. The reactants and products were analyzed using a GC/FID system, which has been described elsewhere.[3] The GC temperature program used in these analyses on a 30 m DB−1 column with 5 μm coating was the following: 35 °C (3 min); 20 °C/min to 65 °C; hold 0.3 min; 38 °C/min to 155 °C and hold. Product identification studies were carried out when necessary using an identical GC equipped with a mass spectrometric detector. The experiments were performed on Cl_2 (99.7%)/CH_4 (research grade)/butanone (99.5%) mixtures in N_2 (UHP) or N_2/O_2 (research) diluent (freeze−thaw−degassing cycles were performed on butanone and Cl_2 reactants). Methane was used for internal calibration of the GC analysis since it is essentially unreactive toward Cl ($k = 1.04$ and 10.2×10^{-13} cm^3 $molecule^{-1}$ s^{-1} at 297 and 526 K, respectively)[4] relative to butanone ($k = 4 \times 10^{-11}$). Ethane (research) was added as a reference compound in selected relative rate experiments to measure the temperature dependence of the overall rate coefficient for reaction 1.

Chlorine atoms were generated by irradiation of the unreacted mixture with UV light using a single Sylvania F6T5 BLB fluorescent lamp. During irradiation, the 500 cm^3 flask was rotated to provide more uniform irradiation. After a chosen irradiation time, a portion of the contents of the reactor was removed into a 2.5 cm^3 gastight syringe and analyzed by direct injection of this sample into the injector port (at 373 K) of the gas chromatograph. The presence of CH_4 as an internal calibrant permitted corrections to be made for uncertainty in the precise amount of sample injected into the GC using the syringe. The mixture was then irradiated for additional times, and additional analyses were performed.

All ambient temperature experiments were carried out at a total pressure of 800−950 Torr. The reactant partial pressure ranges were the following: Cl_2 (700−10 000 ppm); butanone (200−300 ppm); CH_4 (~600 ppm); O_2 (0−200 000 ppm); balance N_2. In addition, an irradiation experiment was performed in the absence of Cl_2 to verify that direct photolysis of butanone does not occur. No photolysis was observed in these experiments.

Elevated temperature experiments were performed over the range 297−526 K using a ~40 cm^3, cylindrical, Pyrex reactor (26 mm i.d. × ~7 cm length) with a thermocouple well along the axis and a Teflon-sealed, glass stopcock attached to a Pyrex capillary tube at the end opposite the thermocouple well. The reactor was placed inside a tube oven, whose lid was open approximately 6 mm to allow radiation from the fluorescent lamp to enter. The calibration of the chromel−alumel thermocouple was checked in ice and boiling water. The temperature along the axis of the reactor was uniform to ~3 K from the mean. During a reaction, a portion of the unreacted mixture was placed into the reactor at pressures varying from 700 to 900 Torr depending on the depletion in the reactant storage flask. The mixture was then irradiated for a chosen time, and the contents were withdrawn into a 100 cm^3 transfer flask outside of the oven. Samples from the 100 cm^3 flask, pressurized to 1 atm with N_2, were injected into the GC using the syringe. Only one irradiation was possible per sample placed into the reactor for the high temperature experiments.

For selected samples, two analyses were performed to assess sample stability, which showed that the samples were always stable in the 100 cm^3 sample flask for >15 min. In addition, mixtures were also placed in the reactor without irradiation to determine the degree of thermal reaction that may occur as the temperature is increased. Significant thermal reaction was observed only at temperatures greater than ~500 K. Analysis of the data indicates that products formed and rate constants measured when thermal reaction is present are consistent with the data in the absence of thermal reaction. Therefore, the thermal reaction also occurs by a Cl chain reaction process whose product yields are indistinguishable from the irradiated mixtures.

At ambient temperature, experiments were performed in the high temperature reactor, in the 0.5 L spherical Pyrex flask, and in an FTIR smog chamber. The product yields were indistinguishable in these three reactors, verifying that surface reactions play no significant role in these measurements.

Product identification and calibration are ideally carried out by injecting a known concentration of the pure product into the GC to determine its FID sensitivity and retention time. This is convenient only if the product is commercially available. Pure samples of many products are available for identification and calibration, including acetaldehyde, acetyl chloride, propionyl chloride, butanedione, and methylvinylketone. Of the three possible chlorobutanone products only 3-chlorobutanone is commercially available to our knowledge. The 1-chloro- and 4-chloro-butanone isomers were identified by their mass spectra using the GC/MS detector as discussed in the Appendix. Direct concentration calibration for these two species was not possible. However, for all species for which pure samples are available (including some chlorinated species which are not present in these experiments such as chloroethane, chlorinated pentanones, and others), the GC sensitivity per mole fraction of the species in the sample was directly proportional to the number of nonoxygenated carbon atoms in the species corrected for a small sample loss in the GC injection system which is approximately proportional to its retention time on the GC column. The sample loss corrections were factors of 1.17 and 1.13 for 4- and 1-chlorobutanone, respectively. The carbonyl groups had no response to the FID detector as verified in these calibration studies.

Butanedione and MVK have identical retention times on the GC column used in these experiments. Therefore, the identity of the compound producing the observed GC peak at this retention time was determined by using the GC/MS instrument. As an example, Figure 11 in the Appendix presents the product mass spectrum from an ambient-temperature, irradiation experiment (black lines) in the presence of O_2, and a spectrum of butanedione (red lines) run as a calibration standard on this GC/MS instrument. The product spectrum is identical to that of the butanedione standard. At temperatures in the range 297−400 K, the experimental spectrum observed after irradiation remained that of butanedione, although the noise level became larger as the temperature increased. At temperatures in excess of 490 K and very high O_2 mole fraction (170 000 ppm), no mass fragment at 86 amu attributable to butanedione is observed above the noise level as shown in Figure 12. This figure presents the mass spectrum at the retention time of the common MVK/butanedione GC peak obtained at 520 K (black lines) and high O_2. The MVK ($CH_3C(O)C_2H_3$) fragmentation pattern (red lines) from the NIST/EPA/NIH Mass Spectral Library (2002) is also included and matches the three major fragments of the unknown product mass spectrum well.

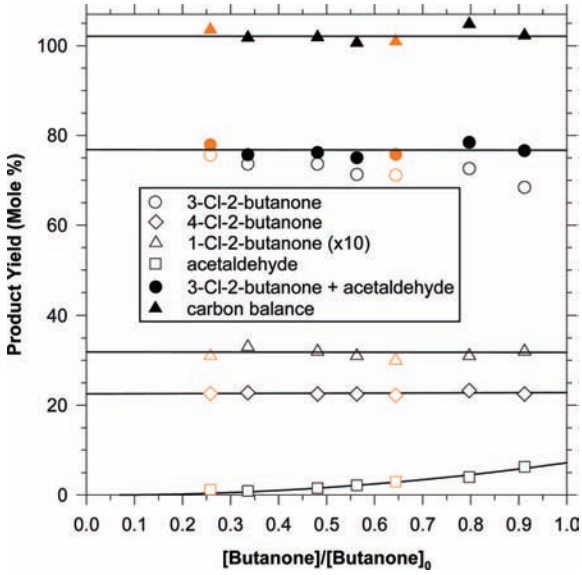

Figure 1. Measured product yields in the 500 cm^3 reactor generated by reaction 1 plotted as a function of butanone consumed in the absence of added O_2. Initial conditions using the GC method (black symbols) for three separate initial mixtures follow: 297 K; 800−950 Torr N_2; Cl_2 = 930 ppm; butanone = 230 ppm; N_2 = balance. Initial conditions for the orange symbols are the same except Cl_2 = 2700 ppm. All species yields have been corrected for secondary consumption by Cl (see text). Also shown are the following: (1) filled circles = the total yield from Cl attack at the 3-position (3-Cl-2-butanone + CH_3CHO), and (2) carbon balance = sum of the molar yields of all products.

Experiments were also carried out at ambient temperature in the presence of O_2 using a smog chamber with FTIR detection of reactants and products, which has been described in detail elsewhere.[2] Briefly, it consists of a 140 L Pyrex chamber with analyses performed by an IR beam which executes multiple passes along the axis of the cylindrical chamber. The spectral analysis is performed by a Mattson FTIR spectrometer. This apparatus was used to cross check the GC studies using a different detector and reactor.

3. Results and Discussion

3.1. Ambient Temperature.

3.1.1. Products Observed in Nitrogen Diluent. Experiments were carried out at ambient temperature in N_2 diluent. In the absence of added O_2, three product peaks were observed in the GC analysis. The 3-chlorobutanone product formed via reaction 2a was identified and calibrated using the commercially available, pure compound. Two other primary product peaks were identified using the GC/MS instrument. One of these peaks was identified as 4-chloro-2-butanone (see the product mass spectrum in the Appendix, Figure 13, compared to that of 4-chlorobutanone from the NIST/EPA/NIH Mass Spectral Library (2002)), while the other was confirmed to be 1-chlorobutanone (see Figure 14).

Figure 1 (black symbols) presents the molar yields of the products plotted as a function of the butanone consumed in the 500 cm^3 reactor (mole of product per mole of butanone consumed) in the absence of added O_2 at a total pressure of 800−950 Torr and initial Cl_2 of 930 ppm. Irradiation times varied from 3 to 20 s. Table 1 (upper section) tabulates the data points from Figure 1 including both measured yields and the yields after correction for secondary consumption by Cl atoms (see below). The initial reactant species mole fractions are also included in this table. The orange symbols are data obtained from an initial mixture having the same butanone mole fraction but with increased Cl_2 (2750 ppm); irradiation times for these data were ∼2.5 and 5.5 s. The two Cl_2 mole fractions give indistinguishable results. The effect of initial pressure was also examined by irradiating an initial mixture similar to those in Figure 1 but with the pressure of N_2 diluent reduced to 125 Torr. These results agree with the higher pressure data to within 10−15%, which is of the order of the experimental error.

The yields of 3-chlorobutanone and CH_3CHO in this figure have been corrected for secondary consumption by Cl atoms using a computer model (Acuchem)[5] and the known rate constants for these species (5.6×10^{-12} and 8×10^{-11} cm^3 $molecule^{-1}$ s^{-1}, respectively[2,6]). The rate constants for Cl reaction with 1-chloro and 4-chlorobutanone are unknown, but the uncorrected yields of these species presented in Table 1 decrease steadily with increasing butanone consumption, falling by factors of (0.64 ± 0.15) and (0.89 ± 0.04), respectively, after 66% of the butanone is consumed. Using the computer model to remove this secondary consumption, approximate values for the rate constants of Cl reaction with the 1-chloro and 4-chlorobutanone isomers were deduced (3×10^{-11} and 7×10^{-12} cm^3 $molecule^{-1}$ s^{-1}, respectively). These rate constants were used to produce the corrected yields for these two species shown in Figure 1 and in Table 1. The value for 1-chlorobutanone is only 25% less than that of butanone itself. Addition of a single Cl to the methyl group in the 1 position might be expected to exert minimal influence on the abstraction of H atoms from the ethyl group on the other side of the carbonyl (note that the rate constant for reaction of Cl with chloroacetone is only 10% smaller than that of Cl with acetone[7]). The rate constant for Cl reaction with 4-chlorobutanone, however, is a factor of ∼6 smaller than that for butanone indicating that the chlorine substituent at the 4-position deactivates the neighboring 3-position. In a similar fashion, the rate constant for reaction of Cl with chloroethane is a factor of ∼7 smaller than that with ethane.[8]

A small yield of CH_3CHO is observed in Figure 1, which decreases as the consumption of butanone increases. The presence of CH_3CHO indicates that there is typically a small, unavoidable O_2 contaminant present in the reaction mixture. The CH_3CHO yield decreases with increasing butanone consumption consistent with the expected removal of most of this small O_2 contaminant early in the reaction. As discussed later, CH_3CHO is the major product of the reaction of O_2 with the $CH_3C(O)CHCH_3$ radical. The molar yield of 3-chlorobutanone expected in the total absence of O_2 (filled circles) is obtained from the sum of its measured yield (open circles) plus the molar yield of CH_3CHO (squares). The yields of 1-chloro-, 3-chloro-, and 4-chlorobutanone in Figure 1 are (3.1 ± 0.6)%, (76 ± 7)%, and (22.5 ± 2.5)% where the error limits include data scatter plus an estimate of the product calibration error. The sum of the product molar yields, presented in Figure 1 as filled triangles, is equal to (102 ± 6)%. The excellent molar product balance provides confirmation that the product calibrations are accurate. The yield of the 3-chlorobutanone agrees well with the value (73 ± 9)% determined by Iwasaki et al.[2]

The measured yields of the chlorobutanones can be combined with the overall rate constant of reaction 1 ($k_1 = 3.8 \pm 0.3 \times 10^{-11}$ cm^3 $molecule^{-1}$ s^{-1})[1] to obtain individual rate constants for eqs 1a, 1b, and 1c [e.g., $k_{1a} = k_1 \times Y$(3-chlorobutanone)] at 297 K. The calculated values are the following: $k_{1a} = 2.9$ (± 0.27) $\times 10^{-11}$; $k_{1b} = 8.6$ (± 1.0) $\times 10^{-12}$; and $k_{1c} = 1.2$ (± 0.24) $\times 10^{-12}$ cm^3 $molecule^{-1}$ s^{-1}. In these expressions, the

TABLE 1: Molar Product Yields (%) per Mole of Butanone Consumed

C/C_0	1-Cl %	3-Cl %	4-Cl %	CH_3CHO %	CH_3COCl %	C_2H_5COCl %	butanedione %	Σ C %
no O_2 added	930 ppm Cl_2	220 ppm	butanone					
0.91	3.1[a]	67.9	22.3	5.7		<0.1[b]	1.9[b]	
	3.2[a]	68.4	22.5	6.3				102.3
0.80	2.8	71.3	22.8	3.4			1.8	
	3.1	72.6	23.3	4.0				104.8
0.56	2.5	68.0	21.2	1.2		~0.1	1.5	
	3.1	71.3	22.5	2.2				100.6
0.48	2.4	69.3	20.9	0.7		~0.1	1.1	
	3.2	73.6	22.5	1.5				101.9
0.34	2.1	66.3	20.3	0.3		~0.1	1.2	
	3.3	73.6	22.8	0.9				101.8
400 ppm O_2	900 ppm Cl_2	218 ppm	butanone					
0.79	0.2 ± 0.15	2.15	18.4	41	67[c]	2.5	11.2	
	0.22 ± 0.15	2.23	18.9	52	56			
0.43	0.2 ± 0.15	1.8	16.6	21	85	2.6	12	
	0.28 ± 0.15	2.0	18.1	52	54			
0.24	<0.3	1.6	15.5	12	95	2.6	12.8	
		1.9	18.2	52	55			

[a] Upper entry = measured yield; lower entry = the yield corrected for secondary consumption of the product by Cl; 1-Cl, 3-Cl, and 4-Cl represent 1-, 3-, and 4-chlorobutanone, respectively. C/C_o = fraction of initial butanone remaining. [b] No correction for secondary consumption required because of the slow rate constant for Cl reaction. [c] Upper entry for CH_3COCl = measured yield; lower entry = measured yield minus correction applied to CH_3CHO to remove secondary consumption [=67 − (52 − 41) = 56%], see text.

error limits represent the relative precision based on the uncertainty in the yields and do not include uncertainty in the value of k_1.

The rate constant for hydrogen abstraction at the methyl group located at the 1 position (k_{1c}) in butanone is nearly identical to that for abstraction at a single methyl group in acetone ($0.5 \times k_{acetone} = 0.5 \times (2.1 \times 10^{-12})^9 = 1.05 \times 10^{-12}$ cm^3 molecule^{-1} s^{-1}). However, it is 0.04 times the typical rate constant for Cl abstraction at a methyl group in an alkane (3.0×10^{-11} cm^3 molecule^{-1} s^{-1}).[10] The rate constant for H atom abstraction at the methyl group in the 4-position in butanone (k_{1b}) is 0.29 times that for an alkane methyl group. The abstraction rate constant at the 3-carbon position (k_{1a}) is 0.38 times that for hydrogen abstraction at a secondary carbon in alkanes (7.7×10^{-11} cm^3 molecule^{-1} s^{-1}).[10] The authors in ref 2 inferred indirectly that the presence of a carbonyl group deactivates the H atoms toward abstraction by Cl atoms on carbons in the α position (forming 1- or 3-chlorobutanone) as well as those in the β position (forming 4-chlorobutanone). The direct determinations of the rate constants for Cl abstraction at the 1, 3, and 4 carbon positions in butanone presented herein confirm the reactivity discussions in ref 2.

3.1.2. Products Observed in N_2/O_2 Diluent. Figure 2 presents the molar product yields obtained following UV irradiation of butanone/Cl_2/O_2/N_2 mixtures in the 500 cm^3 reactor (black symbols). The initial reactant mixture composition was the following: butanone (205−218 ppm), Cl_2 (765−900 ppm), O_2 (320−400 ppm), and a total pressure of N_2 diluent of 800−950 Torr. The red symbols show data obtained using the FTIR reactor system under similar but not identical conditions. Table 1 (lower section) presents representative data from one of the three initial mixtures tested at this initial composition using the GC/FID system. All species yields with the exception of butanedione, with which Cl reacts very slowly (see below), have been corrected for secondary consumption of the species by Cl as discussed above. To demonstrate the accuracy of the computer generated correction for CH_3CHO, the uncorrected data are also presented in Figure 2 (filled squares). The corrected CH_3CHO yields (unfilled squares) are identical to within the data scatter, while the uncorrected yields fall sharply with

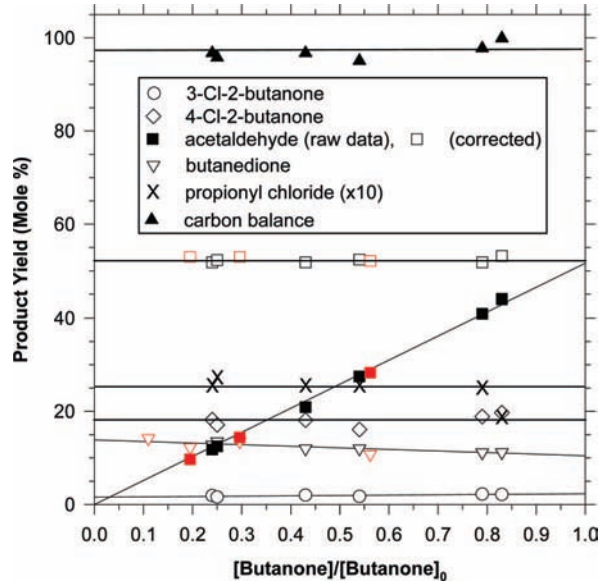

Figure 2. Measured product yields from reaction 1 as a function of butanone consumed in the presence of added O_2. Initial conditions for the GC experiments (black symbols) for three separate initial mixtures: 297 K; 800−950 Torr N_2; Cl_2 = 765, 784, 900 ppm; O_2 = 401, 317, 404 ppm; butanone = 205, 207, 218 ppm; N_2 = balance. Red symbols were measured on the FTIR apparatus with the following initial conditions: 700 Torr; Cl_2 = 1260 ppm; O_2 = 500 ppm; butanone = 42 ppm; N_2 = balance. All species yields except that of butanedione have been corrected for secondary consumption by Cl except the filled squares for CH_3CHO which are uncorrected (see text). Carbon balance = sum of the molar yields of all products from the GC experiments. The yield of 1-chlorobutanone is (0.25 ± 0.12)%.

increasing butanone consumption. As stated in the discussion of the results obtained in the absence of added O_2 (see section 3.1.1), one experiment was also carried out at a total pressure of 125 Torr. These lower-pressure data produced product yields which were indistinguishable from the data in Figure 2 to within the estimated error of 10−20%.

The data in Figure 2 show dramatic changes from the results in the absence of added O_2 presented in Figure 1. Addition of this relatively modest amount of O_2 (~400 ppm) causes the

TABLE 2: Mechanism Used to Model the Experimental Data[a]

eq	reactants	products	rate constant
1a	$Cl + CH_3C(O)CH_2CH_3$	$CH_3C(O)CHCH_3 + HCl$	2.85×10^{-11}
1b	$Cl + CH_3C(O)CH_2CH_3$	$CH_3C(O)CH_2CH_2 + HCl$	$(1.9 \times 10^{-11})(e^{-470/RT})b$
1c	$Cl + CH_3C(O)CH_2CH_3$	$CH_2C(O)CH_2CH_3 + HCl$	$(2.30 \times 10^{-11})(e^{-1800/RT})b$
2a	$CH_3C(O)CHCH_3 + Cl_2$	$CH_3C(O)CHClCH_3 + Cl$	1.13×10^{-14}
2b	$CH_3C(O)CH_2CH_2 + Cl_2$	$CH_3C(O)CH_2CH_2Cl + Cl$	1.52×10^{-12}
2c	$CH_2C(O)CH_2CH_3 + Cl_2$	$CH_2ClC(O)CH_2CH_3 + Cl$	2.70×10^{-14}
3a	$CH_3C(O)CHCH_3 + O_2$	$CH_3C(O)CH(O_2)CH_3$	1.00×10^{-12}
−3a	$CH_3C(O)CH(O_2)CH_3$	$CH_3C(O)CHCH_3 + O_2$	$(5.63 \times 10^{16})(e^{-24500/RT})b$
3b	$CH_3C(O)CH_2CH_2 + O_2$	$CH_3C(O)CH_2CH_2(O_2)$	1.00×10^{-12}
3c	$CH_2C(O)CH_2CH_3 + O_2$	$CH_2(O_2)C(O)CH_2CH_3$	1.00×10^{-12}
−3c	$CH_2(O_2)C(O)CH_2CH_3$	$CH_2C(O)CH_2CH_3 + O_2$	$(4.40 \times 10^{14})(e^{-24500/RT})$
4a	$2CH_3C(O)CH(O_2)CH_3$	$2CH_3C(O)CH(O)CH_3 + O_2$	8.00×10^{-12}
4b	$2CH_3C(O)CH_2CH_2(O_2)$	products + O_2	6.00×10^{-12}
4c	$2CH_2(O_2)C(O)CH_2CH_3$	$2CH_2(O)C(O)CH_2CH_3 + O_2$	5.00×10^{-12}
5a	$2CH_3C(O)CH(O_2)CH_3$	$CH_3C(O)C(O)CH_3 + CH_3C(O)CH(OH)CH_3 + O_2$	$(1.08 \times 10^{-13})(e^{1850/RT})b$
6ab	$CH_3C(O)CH(O_2)CH_3 + CH_3C(O)CH_2CH_2(O_2)$	$CH_3C(O)C(O)CH_3$ + product + O_2	$(1.96 \times 10^{-13})(e^{1850/RT})b$
7a	$CH_3C(O)CH(O)CH_3$	$CH_3C(O) + CH_3CHO$	fast (1×10^{12})
7c	$CH_2(O)C(O)CH_2CH_3$	$CH_2O + CH_3CH_2C(O)$	*c*
8	$CH_3C(O) + O_2$	products	4.00×10^{-12}
9	$CH_3CO + Cl_2$	$CH_3C(O)Cl + Cl$	3.00×10^{-11}
10	$CH_3CH_2C(O) + Cl_2$	$CH_3CH_2C(O)Cl + Cl$	*c*
11	$CH_3C(O)CH(O_2)CH_3$	$CH_3C(O)C_2H_3$ [MVK] + HO_2	$(2.75 \times 10^{11})(e^{(-22500/RT)})$

[a] Units are cm^3 $molecule^{-1}$ s^{-1}, cal, K. ($R = 1.986$ cal K^{-1} $mole^{-1}$). [b] Rate constant derived partially from the current data but include some estimation. All other rate constants are estimates based similar types of reactions available in the literature. For detailed discussions concerning the choices made, see section 4.0 as well as other sections in the text. [c] Not included in model but discussed as the source of propionyl chloride observed under selected initial conditions (see text).

3-chlorobutanone yield to decrease from 76% in N_2 to 2%. The 1-chlorobutanone yield is not plotted but decreases from 3.1% to ~0.25 (±0.12)% as presented in Table 1. The 4-chlorobutanone also decreases but by a much smaller amount (22.5% in N_2 to 18.5% with O_2 present). Finally, four oxygenated products appear [52 mol % CH_3CHO, 11% butanedione, 2.5% C_2H_5COCl, and ~52% CH_3COCl (see Table 1)]. The initial molar yield of CH_3COCl [formed by reaction of the acetyl radical with Cl_2 (reaction 9 in Table 2)] is approximately equal to that of CH_3CHO but increases as the butanone consumption increases because it is also formed from the secondary consumption of CH_3CHO. Table 1 presents the measured CH_3COCl (top entry) and its yield after correction for CH_3COCl formation from secondary consumption of CH_3CHO (bottom entry). Acetyl chloride is not included in Figure 2 to reduce the clutter of data points because CH_3CHO provides similar information as discussed below. Butanedione has a low reactivity toward chlorine atoms ($k = 4.0 \times 10^{-13}$ cm^3 mol^{-1} s^{-1}),[11] and no correction for secondary consumption is applied. In fact, the yield of butanedione actually increases as the butanone consumption increases (see Table 1 and Figure 2). On the basis of the data in Figure 2, this modest increase might seem to be simply data scatter. However, the effect is observed in every individual series of measurements including those using the FTIR reactor.

The yields of butanedione, acetaldehyde, and 3-chlorobutanone measured using the FTIR/smog chamber system (red data points in Figure 2) are indistinguishable data obtained from the GC measurements. In addition, the upper limit to the yield of 3-chlorobutanone (<2%) is again consistent with the GC data. The fact that the measured yields in very different reactors are consistent with one another provides evidence that heterogeneous processes do not play a significant role in the chemical mechanism. The indistinguishable butanedione yields in the GC and FTIR experiments also provide additional confirmation that the GC peak identified as butanedione using GC/MS analysis is, in fact, butanedione.

The oxygenated products observed in Figure 2 can be explained by the chemical mechanism in Table 2 which accounts for reactions following the formation of peroxy radicals [M is a third body (e.g., N_2 diluent) which removes the internal excitation in the nascent peroxy radical].

$$CH_3C(O)CHCH_3 + O_2 + M \rightarrow CH_3C(O)CH(O_2)CH_3 + M \quad (3a)$$

$$CH_3C(O)CH_2CH_2 + O_2 + M \rightarrow CH_3C(O)CH_2CH_2O_2 + M \quad (3b)$$

$$CH_2C(O)CH_2CH_3 + O_2 + M \rightarrow CH_2(O_2)C(O)CH_2CH_3 + M \quad (3c)$$

The 3-butanonylperoxy radical ($CH_3C(O)CH(O_2)CH_3$) formed in reaction 3a can react with itself via reactions 4a and 5a to form the 3-butanonoxy radical ($CH_3C(O)CH(O)CH_3$) or butanedione plus 3-hydroxybutanone, respectively:

$$2\ CH_3C(O)CH(O_2)CH_3 \rightarrow 2\ CH_3C(O)CH(O)CH_3 + O_2 \quad (4a)$$

$$2\ CH_3C(O)CH(O_2)CH_3 \rightarrow CH_3C(O)C(O)CH_3 + CH_3C(O)CH(OH)CH_3 + O_2 \quad (5a)$$

It can also react with other peroxy radicals, particularly 4-butanonylperoxy. The 3-hydroxybutanone is likely to undergo secondary consumption by Cl primarily via H abstraction at the carbon to which the OH is attached followed by reaction with O_2 to form butanedione by analogy to the reaction Cl + C_2H_5OH:[12]

$$CH_3C(O)CH(OH)CH_3 + Cl = CH_3C(O)C(OH)CH_3 + HCl \quad (A)$$

$$CH_3C(O)C(OH)CH_3 + O_2 = CH_3C(O)C(O)CH_3 + HO_2 \quad (B)$$

This reaction sequence would form butanedione as a secondary product, explaining the rise in butanedione concentration in Figure 2 as the percentage consumption of butanone increases. The observed secondary generation was reproduced and corrected for using computer modeling with a rate constant for reaction A of 7×10^{-12} cm^3 molecule^{-1} s^{-1} to give an estimate of the primary yield of butanedione (11% in Figure 2).

Figure 3 presents the effect of changing the O_2 mole fraction (with Cl_2 = 700−900 ppm) on the yields of the major products at 297 K in the 500 cm^3 reactor. Initial reactant mole fractions for each data point are shown in the caption. Adding 400 ppm of O_2 sharply reduces the 3-chlorobutanone yield from 76% to 2% while the CH_3CHO yield simultaneously rises sharply from 0% to ∼53%. After this initial rise, the yield of acetaldehyde remains nearly constant as more O_2 is added, while the 3-chlorobutanone continues to decrease from 2% to 0% within experimental error. The 4-chlorobutanone yield decreases only modestly upon addition of 400 ppm of O_2 (from 22.5% to 18.5%) but continues to decrease as more O_2 is added until its yield also nears 0% between 11 000 and 200 000 ppm. The yield of butanedione (corrected by removal of the secondary formation as described above) initially rises sharply to a yield of ∼11% upon addition of 400 ppm of O_2. This rise is followed by a much slower increase as the O_2 increases to 11000 ppm. No further increase in butanedione yield occurs as the O_2 mole fraction increases to 200 000 ppm. The yields of butanedione and acetaldehyde measured using the FTIR system (Cl_2 = 1250 ppm) are presented in this figure as red symbols. Both the yields

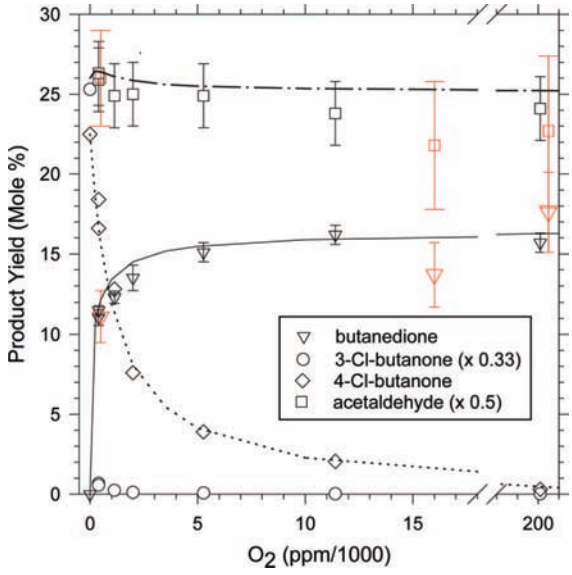

Figure 3. Product yields plotted as a function of the O_2 mole fraction. Initial conditions for eight initial mixtures using the GC method (black symbols) follow: P = 800−950 Torr in N_2; 297 K; Cl_2 = 923, 897, 765, 823, 682, 689, 686, 689 ppm; O_2 = 0, 404, 401, 1135, 2000, 5279, 11 400, 202 000 ppm; butanone = 236, 218, 205, 222, 206, 233, 202, 212 ppm; N_2 = balance. Initial conditions for three initial mixtures using the FTIR method (red symbols) follow: P = 700 Torr; Cl_2 = 1260, 1300, 1280 ppm; O_2 = 500, 16 000, 210 000 ppm; butanone = 42, 42, 42 ppm; N_2 = balance.. All species yields have been corrected for secondary consumption by Cl (see text). Butanedione has been corrected for its formation via secondary consumption of 3-hydroxy-2-butanone (see text). Curves are derived from the mechanism in Table 2 (see text).

and the trends of the FTIR data are consistent with the GC data. However, the estimated precision of the FTIR data is not as good as the GC data because of overlapping spectral bands among the reactants/products and the relatively weak band strengths of the broad product peaks. The error limits include uncertainties in the spectral deconvolution. The error bars for butanedione using GC analysis represent the estimated precision of the measurements and do not include uncertainty in the calibration since calibration error will not affect the observed trend with O_2 partial pressure.

The data in Figure 3 are important to understanding the mechanism of butanedione formation. The 3-butanonoxy radical can decompose via C−C bond scission to yield CH_3CHO and CH_3CO (reaction 7a), or it could react with O_2 to form butanedione by reaction C:

$$CH_3C(O)CH(O)CH_3 \rightarrow CH_3CHO + CH_3CO \quad (7a)$$

$$CH_3C(O)CH(O)CH_3 + O_2 \rightarrow CH_3C(O)C(O)CH_3 + HO_2 \quad (C)$$

If reaction C is important in the mechanism, it would be expected that increasing the O_2 mole fraction at constant Cl_2 would lead to a steadily increasing yield of butanedione. Concurrently, the yield of CH_3CHO from reaction 7a would decrease until the major product observed from 3-butanonoxy radicals would be butanedione with little, or no, formation of CH_3CHO. Inspection of Figure 3 shows that this is not what is observed. Addition of ∼400 ppm of O_2 causes a sharp rise in the yields of both butanedione and acetaldehyde accompanied by a very sharp, large decrease in the 3-chlorobutanone yield as the consumption of 3-butanonyl radical becomes dominated by O_2 addition (reaction 3a). During this initial sharp change, the 3-chlorobutanone yield decreases from 76% to 2%. At the same time, the CH_3CHO increases from 0% to 53%, and the butanedione yield rises from 0% to 11%. As the O_2 mole fraction continues to increase, little decrease occurs in the CH_3CHO yield and butanedione rises only a small amount (from 11.5% to 16.5%). The fact that CH_3CHO is not suppressed at very high [O_2] indicates that little measurable butanedione is formed by reaction C under these experimental conditions. This observation is consistent with an experimental and theoretical study of the acetonoxy radical in which decomposition to form formaldehyde and an acetyl radical by a reaction analogous to 7a in the butanone experiments is the only reaction channel open even in the presence of 1 atm of O_2.[13] Thus, butanedione is likely formed by the self-reaction 5a at moderate O_2 mole fractions (∼400 ppm). For every butanedione formed by reaction 5a, there will also be one 3-hydroxybutanone created, which could not be identified in the GC analysis. Assuming that 5a is the major source of butanedione at 400 ppm of O_2, all three species (CH_3CHO, butanedione, and 3-hydroxybutanone) arise from reactions of the 3-butanonyl radical. Because the yield of 3-hydroxybutanone must equal that of butanedione, the sum of the molar yields of these three oxygenated products plus that of 3-chlorobutanone (CH_3CHO + $CH_3C(O)C(O)CH_3$ + $CH_3C(O)CH(OH)CH_3$ + $CH_3C(O)CHClCH_3$ = 53 + 11 + 11 + 2) equals 77%. This is identical within experimental error to the yield of 3-chlorobutanone formed in the absence of added O_2 (=76%, see Figure 1) providing support for this portion of the proposed mechanism. It also indicates that the initial yield of 3-butanonyl radicals is identical in the presence and absence of O_2.

The sum of the yields of propionyl chloride (2.5%) in Figure 2 and 1-chlorobutanone (∼0.25% in Table 1) is equal to the

yield of 1-chlorobutanone in the absence of added O_2 (3.1%) within experimental error. Propionyl chloride is formed by reaction of Cl_2 with propionyl radicals in the presence of relatively small quantities of O_2 as discussed for the acetyl radical earlier (see reaction 10 in Table 2). This indicates that decomposition of the 1-butanonoxy radical to form CH_2O and a propionyl radical via reaction 7c in Table 2 is the major reaction path for this alkoxy radical in the presence of O_2, similar to reaction 7a for 3-butanonoxy radicals. No products from oxidation of 4-butanonyl radicals have been identified.

After the initial sharp rise, the butanedione yield in Figure 3 continues to increase with increasing O_2 but only by approximately 5% in yield. This continued increase in butanedione over the O_2 range 400−11 000 ppm occurs at a much slower rate which is similar to the rate of decrease in 4-chlorobutanone. The simplest explanation is that this increase arises from a cross reaction (eq 6ab) between 3- and 4-butanonylperoxy radicals, which will become important only as the 4-butanonyl radical begins to be consumed significantly by O_2 addition (3b) as indicated by the reduction in yield of 4-chlorobutanone. This will increase the concentration of the 4-butanonylperoxy ($CH_3C(O)CH_2CH_2O_2$) radical.

$$CH_3C(O)CH(O_2)CH_3 + CH_3C(O)CH_2CH_2O_2 \rightarrow CH_3C(O)C(O)CH_3 + \text{products} + O_2 \quad (6ab)$$

Not all possible paths for reaction 6ab or similar cross reactions with the 1-butanonylperoxy are presented in Table 2 because reaction 6ab serves the purpose of explaining the observed data and none of these rate constants have been measured to our knowledge. The lines in Figure 3 are derived by applying the mechanism in Table 2 with initial conditions P = 900 Torr; Cl_2 = 750 ppm; butanone = 200 ppm. The data are fitted reasonably well. The rate constants in Table 2 are not necessarily accurate values, but the quality of the predicted fits does provide confirmation that the proposed mechanism is a plausible explanation of the observed oxygen dependence of the product yields particularly butanedione formation in Figures 2 and 3.

3.1.3. Values of k_{2a}/k_{3a}, k_{2b}/k_{3b}, and k_{2c}/k_{3c}. Addition of O_2 reduces the yield of the butanonyl chlorides as discussed above. Data obtained while varying the Cl_2/O_2 ratio were used to obtain the rate constant ratios for the reaction of each of the butanonyl radicals with Cl_2 relative to that with O_2 (k_{2x}/k_{3x}). The expression that allows these ratios to be determined is derived as follows. The definitions of the terms follow: [3RCl(O_2)] = the concentration of 3-chlorobutanone formed in the presence of O_2; [3RCl(N_2)] = the concentration of 3-chlorobutanone formed in the absence of O_2; [3RO_2] = products formed from 3-butanonylperoxy radicals generated via reaction 3a, which is irreversible at ambient temperature; [3R] = 3-butanonyl radical concentration; and t = reaction time. On the basis of standard kinetics equations using reactions 2a and 3a as an example, the following equations are derived: $[3RCl(O_2)] = k_{2a}[3R][Cl_2]t$, $[3RO_2] = k_{3a}[3R][O_2]t$, or $[3RCl(O_2)]/[3RO_2] = \{k_{2a}[Cl_2][3R]t/k_{3a}[O_2][3R]t\} = k_{2a}[Cl_2]/k_{3a}[O_2]$.

Because the fraction of the butanone consumed by Cl to form the 3-butanonyl radical is the same in the presence or absence of O_2 (see the discussion in section 3.1.2), the following equation is derived: [3RO2] = [3RCl(N_2)] − [3RCl(O_2)]. Substituting this equality into the equation above, the following is obtained: $k_{2a}[Cl_2]/k_{3a}[O_2] = [3RCl(O_2)]/\{[3RCl(N_2)] - [3RCl(O_2)]\} = \{([3RCl(N_2)]/[3RCl(O_2)]) - 1)\}^{-1}$.

This equation can be expressed in terms of the measured yield of 3-chlorobutanone in the presence and absence of added O_2 [Y3RCl(O_2) and Y3RCl(N_2)] by dividing the concentrations in the numerator and denominator of the middle expression in the above equation by the butanone consumed to give $\{([Y3RCl(N_2)]/[Y3RCl(O_2)]) - 1\}^{-1} = k_{2a}[Cl_2]/k_{3a}[O_2]$.

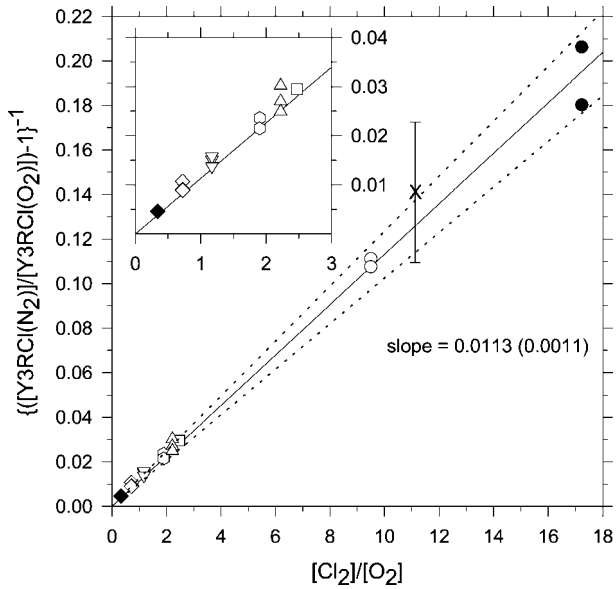

Figure 4. Plot to determine the rate constant ratio k_{2a}/k_{3a} (=0.0113 ± 0.0011). Each symbol represents a separate initial mixture. Multiple data having the same symbol represent different fractional butanone consumption with that mixture. Data shown by the symbol × were obtained from the FTIR apparatus; all other symbols were obtained using the GC method. Range of initial conditions (N_2 balance) for the GC data follows: P = 800−950 Torr; T = 297 K; Cl_2 = 682−10 526 ppm; O_2 = 317−2000 ppm; butanone = 205−239 ppm. Initial conditions for FTIR data (N_2 balance) follow: P = 700 Torr; T = 296 K; Cl_2 = 5586 ppm; O_2 = 500 ppm; butanone = 45 ppm.

Plotting the left side of this equation versus $[Cl_2]/[O_2]$ will yield a straight line whose slope is k_{2a}/k_{3a}. Figure 4 presents such a plot for the 3-butanonyl radical. Each set of symbols represents measurements at the $[Cl_2]/[O_2]$ ratio indicated using one initial mixture with butanone consumption varying from 20% to 75%. The symbol × is the data point obtained using the FTIR/smog chamber apparatus. A linear least-squares fit to the data (using [Y3RCl(N_2)] = 76%, see Figure 1) gives the ratio k_{2a}/k_{3a} = 0.0113 (±0.0011). This is in good agreement with the value of ∼0.01 deduced by Iwasaki et al.[2] Figure 5 (with [Y4RCl(N_2)] = 22.5%) and Figure 6 (with [Y1RCl(N_2)] = 3.1%) present similar plots for the 4- and 1-butanonyl radicals, respectively. The rate constant ratios derived from these plots are the following: k_{2b}/k_{3b} = 1.52 (±0.32) for the 4-butanonyl radical, and k_{2c}/k_{3c} = 0.027 (±0.0035) for the 1-butanonyl radical.

The rate constant ratio k_{2b}/k_{3b} (=1.5) for the 4-butanonyl radical is very similar to the ratios of the rate constants for reaction with Cl_2 to that with O_2 measured for primary sites in alkyl radicals such as methyl,[14] ethyl,[15] and *n*-butyl[10] radicals [2, 2, 3, respectively] at ambient temperature and pressure. However, the ratio for the 1-butanonyl radical (0.027) is a factor of ∼100 smaller. The ratio for the secondary carbon radical, 3-butanonyl, is a factor of ∼300 smaller than that measured for the *sec*-butyl radical (k_{Cl2}/k_{O2} = 3).[10] The smaller ratios observed for the radical position α to the carbonyl group are likely caused by a reduction in the rate constant for reaction with Cl_2 rather than by an increase in the rate constant with O_2 because the measured rate constant[16−18] for the acetonyl ($CH_3C(O)CH_2$) radical reaction with O_2 is ∼1 × 10^{-12} cm^3

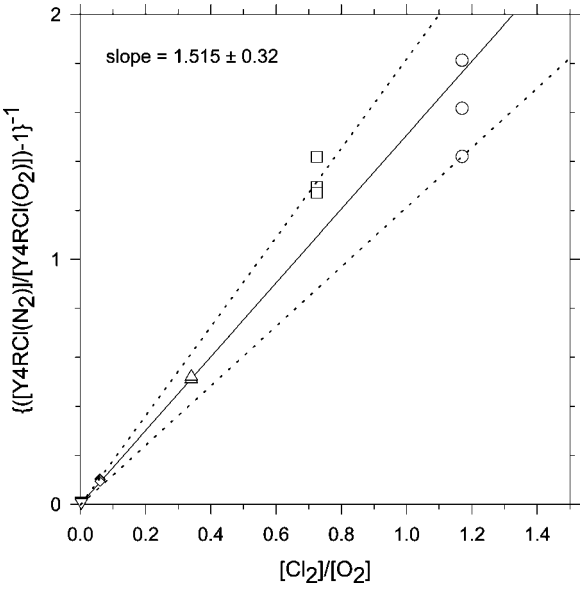

Figure 5. Plot to determine the rate constant ratio k_{2b}/k_{3b} (=1.515 ± 0.32). Each symbol represents a separate initial mixture using the GC method. Multiple data having the same symbol represent different fractional butanone consumption with that mixture. Ranges of initial conditions (N_2 balance) follow: P = 800−950 Torr; T = 297 K; Cl_2 = 682−2290 ppm; O_2 = 0 and 1135−202 000 ppm; butanone = 202−239 ppm.

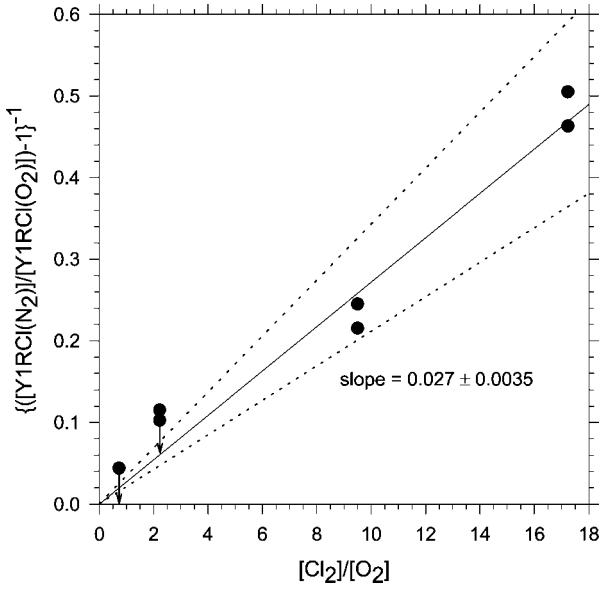

Figure 6. Plot to determine the rate constant ratio k_{2c}/k_{3c} (=0.027 ± 0.0035). Each symbol represents a separate initial mixture using the GC method. Multiple data having the same symbol represent different fractional butanone consumption with that mixture. Ranges of initial conditions (N_2 balance) follow: P = 800−950 Torr; T = 297 K; Cl_2 = 823−10 526 ppm; O_2 = 0 and 369−1135 ppm; butanone = 210−238 ppm. Downward arrows indicate points that are upper limits.

molecule^{-1} s^{-1}. This is of the order of the high pressure limiting rate constant for the reaction of O_2 with the CH_3 radical[14] and only a factor of 5−10 smaller than those for larger alkyl radicals.[9] Assuming that k_{3a}, k_{3b}, and k_{3c} have similar values to that of the acetonyl radical, the rate constants for reaction of 3- and 1-butanonyl radicals with Cl_2 would be $k_{2a} \sim 1$ and $k_{2c} \sim 3 \times 10^{-14}$ cm^3 molecule^{-1} s^{-1}, respectively. These values are much smaller than those measured for C_2−C_4 alkyl radical reactions with Cl_2, which typically have rate constants ranging from 2 to 5 × 10^{-11}.[19] In contrast, the estimated rate constant for the reaction of Cl_2 with the 4-butanonyl radical is substantially larger (∼1.5 × 10^{-12}). It is also possible that the rate constant (k_{3b}) for O_2 addition to the 4-butanonyl radical may be larger than that for addition to 1- and 3-butanonyl radicals since it is farther removed from the carbonyl group. This would increase the estimated value of k_{2b}. These results indicate that the butanonyl radicals α to the carbonyl group are significantly deactivated toward Cl_2 reaction, while the β position retains a more normal Cl_2 reactivity.

3.2. Temperature Dependence.

3.2.1. $k_1(Cl+CH_3C(O)C_2H_5)$. The rate of the reaction of chlorine atoms with butanone was measured relative to the reaction with ethane at 297−475 K in 700−900 Torr of N_2 diluent. Measured rate constant ratios are given in Table 3. The relative rate data were placed on an absolute basis using $k_{C2H6} = (7.23 \times 10^{-13})T^{0.7}[\exp(117/T)]$ cm^3 molecule^{-1} s^{-1} as evaluated by Bryukov et al.[20] Figure 7 shows an Arrhenius plot of the results from the present work (filled circles). The error bars represent the experimental precision based on the scatter in the 2−4 points measured at each temperature and do not include uncertainty in k_{C2H6}. The data at 297 and at 474 K were obtained with no added O_2 while those at 382 and 476 K contained 500 ppm of O_2 in the unreacted mixture. Addition of 500 ppm of O_2 does not change the rate constant at high temperature based on the two data points near 475 K obtained with and without added O_2. Addition of O_2 also does not change the value of k_1 at 297 K.[1,2] As seen from Figure 7, there is no discernible effect of temperature on k_1 and we choose to quote a temperature independent value of $k_1 = (4.0 \pm 0.3) \times 10^{-11}$ cm^3 molecule^{-1} s^{-1} at 297−475 K.

The value of $k_1 = (4.1 \pm 0.2) \times 10^{-11}$ cm^3 molecule^{-1} s^{-1} at 297 K in Figure 7 from the current experiments agrees with the relative rate measurements reported in ref 1 at ambient temperature (3.8 (±0.3) × 10^{-11} cm^3 molecule^{-1} s^{-1}) using propane as the reference species. Data from two other determinations of the temperature dependence of k_1[21,22] are presented in Figure 7. Over the range in which the data overlap (297−386 K), all three sets of data agree reasonably well within the likely combined experimental uncertainties, with the current data lying 10−15% higher than the others. Our data extend the temperature range of the measurements to 475 K, and in the current determination, there is no measurable temperature dependence to within the experimental precision [$E_a(k_1) = 0 \pm 200$ cal mol^{-1}].

3.2.2. Products in N_2 Diluent. Figure 8 presents the measured yields of the 1-, 3-, and 4-chlorobutanones as a function of the reactor temperature in the absence of added O_2. Each data point represents the average of 2−3 measurements having different fractional butanone consumption. The data point at ambient temperature is obtained from experiments in the 500 cm^3 reactor rather than the high temperature reactor because the O_2 contamination observed in the high temperature reactor at ambient temperature was larger than that in the 500 cm^3 reactor. The measured yields of 1- and 3-chlorobutanone have been corrected for the formation of small quantities of oxygenated products (propionyl chloride and acetaldehyde, respectively) caused by unavoidable O_2 contamination (see discussion in sections 3.1.1 and 3.1.2). These corrections are small in both cases, typically increasing the measured yields by a factor of ∼1.05. In the absence of high temperature data, corrections for secondary consumption of the three chlorobutanones were computed using the same rate coefficients employed at 297 K, which provided yields which are independent of the fraction of butanone consumed to within the experimental data scatter. One

TABLE 3: Rate Constant of Reaction 1 (Cl + butanone) Relative to That of C_2H_6 as a Function of Temperature[a]

T (K)	C/C_0	$k/k(C_2H_6)$	$[k/k(C_2H_6)]_{average}$	$k(C_2H_6)$[d]	k[d]
476[b]	0.89, 0.77, 0.46	0.572, 0.592, 0.584	0.58 ± 0.03	6.92	4.0 ± 0.2
474	0.91, 0.81, 0.72, 0.59	0.502, 0.579, 0.597, 0.562	0.56 ± 0.03	6.91	3.9 ± 0.2
382[b]	0.75, 0.54, 0.40	0.629, 0.643, 0.631	0.634 ± 0.03	6.30	4.0 ± 0.2
297[c]	0.81, 0.56	0.701, 0.708	0.705 ± 0.03	5.77	4.1 ± 0.2

[a] C/C_0 = fractional consumption of butanone; individual rate constant ratios listed in order of C/C_0. Initial mole fractions unless stated otherwise: ethane = 70 ppm; butanone = 280 ppm; Cl_2 = 1230 ppm; O_2 = none added. [b] 500 ppm O_2 in initial mixture. [c] Initial butanone = 450 ppm. [d] Units are 10^{-11} cm^3 molecule^{-1} s^{-1}; error limits are estimated uncertainty in $k/k(C_2H_6)$ only. For the expression for $k(C_2H_6)$, see text.

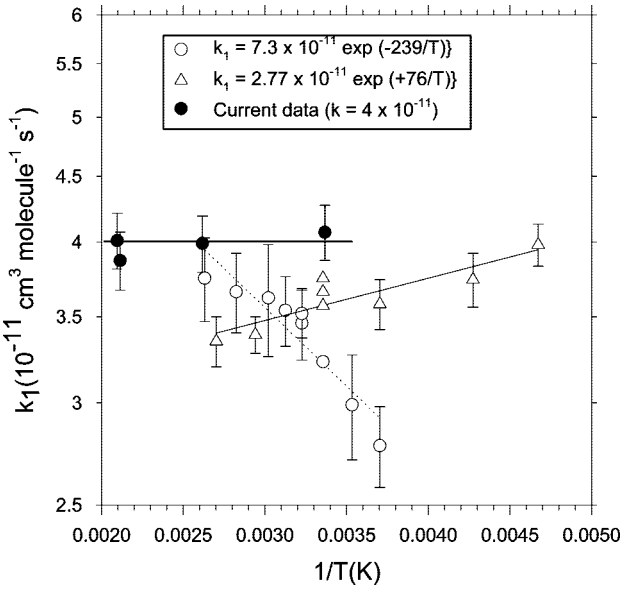

Figure 7. Plots of k_1 (on a $\log_{10}$ scale) as a function of $1/T$. Filled circles are current data using GC analysis. Initial conditions (N_2 balance) for all data follow: Cl_2 = 1222−1256 ppm; butanone = 282−446 ppm; ethane = 62−70 ppm; O_2 = 0 (at 297 and 476 K), 520 ppm (at 382 and 474 K). Open circles are data from ref 22. Triangles are data from ref 21.

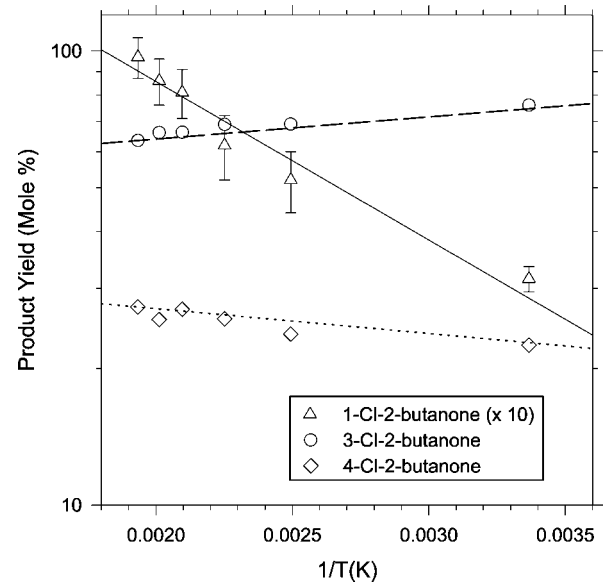

Figure 8. Product yields (corrected for secondary consumption by Cl atoms) plotted as a function of $1/T$. Initial conditions (N_2 balance) follow: P = 700−900 Torr; Cl_2 = 900−1400 ppm; O_2 = 0; butanone = 260−280 ppm. Data at 297 K obtained from Figure 1 in 500 cm^3 reactor. Curves are derived from the mechanism in Table 2 (see text).

additional uncertainty is present in the measurement of the 4-chlorobutanone yield. Sampling from the high temperature reactor may result in a loss of up to ∼20% of this species relative to the measurements at 298 K, which could lead to an underestimate of the temperature dependence. Because this loss was difficult to quantify accurately, no correction for this loss was made in Figure 8, but it was included in the error limits for the estimated activation energy of this isomer.

There is a substantial positive temperature coefficient to the 1-chlorobutanone yield, which increases by a factor of 3 over the range 297−517 K. The yield of 4-chlorobutanone exhibits a much smaller increase in yield of a factor of ∼1.2 over this temperature range. The yield of the 3-chlorobutanone decreases reflecting the increase in yields of the other isomers. The fact that the yield of 1-chlorobutanone exhibits the largest temperature coefficient is consistent with the fact that at 297 K the value of k_{1c} (=1.2 × 10^{-12}) is much smaller than the values of k_{1b} (= 8.6 × 10^{-12}) or k_{1a} (=2.9 × 10^{-11} cm^3 molecule^{-1} s^{-1}). The low value of k_{1c} is likely caused by the fact that reaction 1c has a higher activation energy and may be endothermic, while reaction 1b is much less endothermic, and 1a is nearly thermoneutral. An attempt to estimate the actual activation energy of reaction 1a could be made using the data in Figures 7 and 8. However, because of the small temperature dependence of the yield of 3-chlorobutanone shown in Figure 8 and the small but significant uncertainty in the temperature dependence of k_1 among the three sets of data in Figure 7, we did not choose to pursue such a calculation. By using the Acuchem computer program[5] to simulate the data in Figure 8, estimates of the activation energies of the rate constants for reactions 1b and 1c are derived assuming that the activation energy of reaction 1a is zero. Under this latter assumption, the activation energies for reactions 1b and 1c are calculated to be 470 (+300, −150) and 1800 (±300) cal/mol, respectively. The error in 1b includes the additional sampling uncertainty in the high temperature reactor discussed in the preceding paragraph. These rate constants are included in Table 2 with A factors deduced from the activation energies combined with the absolute values of k_{1b} and k_{1c} at 297 K presented in section 3.1.1. The activation energy calculated for reaction 1c is very similar to that measured by Orlando et al.[13] for the reaction of Cl with acetone (1690 ± 300 cal mol^{-1}). The lines in Figure 8 are the yields generated by Acuchem using these temperature dependent rate constants for the three channels of reaction 1. The activation energies for abstraction of the primary hydrogens in butanone are substantially greater than those observed for ethane (200 cal mol^{-1}) and for the primary (180 cal mol^{-1}) or secondary (−150 cal mol^{-1}) hydrogens in propane.[9]

3.2.3. Products Formed in the Presence of Low Concentrations of O_2. In Figure 9, measured product yields in the high temperature reactor are plotted as a function of $1/T$ for temperatures from 297 to 526 K in the presence of ∼500 ppm O_2 at total pressures of 700−900 Torr. As discussed in section 3.1.2, addition of this relatively small amount of O_2 at 297 K

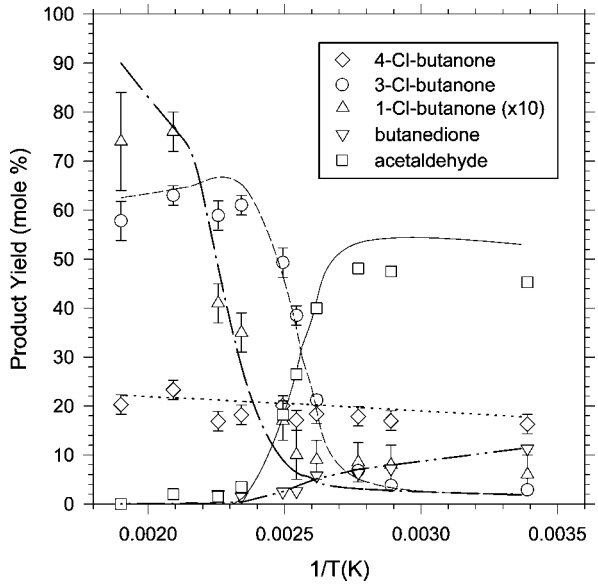

Figure 9. Product yields, corrected for secondary consumption by Cl (see text), plotted as a function of $1/T$. Initial conditions (N_2 balance) follow: $P = 700-900$ Torr; $Cl_2 = 1200-1300$ ppm; $O_2 = 510$ ppm; butanone = 280 ppm. Curves are derived from the mechanism in Table 2 (see discussion in text).

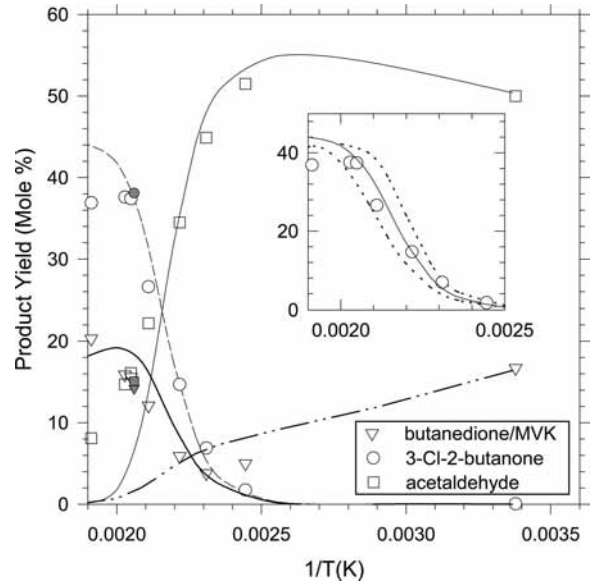

Figure 10. Product yields, corrected for secondary consumption by Cl (see text), plotted as a function of $1/T$. Initial conditions (N_2 balance) follow: $P = 700-900$ Torr; $Cl_2 = 1230$ ppm; $O_2 = 170\,000$ ppm; butanone = 300 ppm. Curves are derived from the mechanism in Table 2 (see discussion in text). The filled data points were obtained at a total pressure of 150−170 Torr of O_2 with no N_2 added.

causes a sharp decrease in the yields of both 1- and 3-chlorobutanone, nearly suppressing these species totally, while the acetaldehyde and butanedione yields increase to ~50% and 11%, respectively. The yield of 4-chlorobutanone decreases modestly from its value in the absence of added O_2.

As the reactor temperature increases, profound changes occur in the product yields. Beginning near 370 K ($1/T = 0.0027$), the yield of 3-chlorobutanone begins to rise, while that of acetaldehyde starts to decrease. By 425 K ($1/T = 0.00235$), the yields of these species are ~60% and ~3%, respectively, and butanedione has also decreased to near zero. The halfway point in the rise of 3-chlorobutanone is ~390 K ($1/T = 0.00256$). The rapid increase in the 3-chlorobutanone concentration accompanied by a decrease in oxygenated products (acetaldehyde and butanedione) originating from the 3-butanonyl radical indicates that the equilibrium concentrations from the oxygen addition reaction (reactions 3a, −3a) are being driven back toward the reactants to a significant degree as the temperature increases from 370 to 425 K. The reversal of this equilibrium raises the concentration of the 3-butanonyl radical relative to the 3-butanonylperoxy radical, thereby reducing the probability of trapping this species as oxygenated products. As reaction 3 becomes reversible, the formation of oxygenated products via $RO_2 + R'O_2$ reactions becomes less probable than reaction of 3-butanonyl with Cl_2. At a sufficiently high temperature, reaction 2a to form 3-chlorobutanone becomes the dominant product path and the mole fractions of butanedione and acetaldehyde decrease to zero within experimental error. A similar effect is observed for 1-chlorobutanone, although the rise begins at a higher temperature (midpoint ~435 K) than that for 3-chlorobutanone. The yield of 4-chlorobutanone increases slowly because of the activation energy of reaction 1b as discussed above. At 400 K, one set of experiments was performed at reduced pressure (125 Torr). These results at reactant partial pressures similar to those in Figure 9 are indistinguishable from the data in Figure 9 to within experimental error.

3.2.4. Products Formed in the Presence of a High Concentration of O_2. The product yields in Figure 10 were measured as functions of temperature in the presence of ~170 000 ppm of O_2. The temperature dependences of the acetaldehyde and 3-chlorobutanone yields show behavior similar to those observed in the presence of 500 ppm O_2. However, the rise in the 3-chlorobutanone yield and the fall in the acetaldehyde yield occur at a higher temperature. The midpoint of the rise in 3-chlorobutanone yield is ~455 K ($1/T = 0.0022$) rather than ~390 K as observed with addition of 500 ppm of O_2. As might be expected, addition of more O_2 pushes the equilibrium of reaction 3 to the right (toward the peroxy radical), and a higher temperature is required to cause the reverse reaction to become important in the mechanism. The yields of both the 1-chloro- (~0.5%) and 4-chlorobutanones (~1%) remain near the detection limit at the higher oxygen mole fraction throughout the temperature range, indicating that reactions 3b and 3c have not become reversible to an extent sufficient to affect the product yields.

The butanedione yield decreases as the temperature increases from 297 to 400 K. However, beyond 435 K ($1/T = 0.0023$), the signal at the retention time for the coeluting butanedione/MVK GC peak actually begins to increase. As discussed in section 2, butanedione and methylvinylketone have the same retention time on the GC column, but GC/MS experiments at high O_2 mole fraction identified butanedione as the only species present at 297 and 395 K (see Figure 11). However, above 490 K, only MVK is observed as shown in the mass spectrum of the combined product peak at 520 K in Figure 12 of the Appendix. This mass spectrum proves that the increasing signal at this retention time at the highest temperatures in Figure 10 results from the presence of a new reaction channel which forms MVK. No butanedione is present to within experimental error based on the absence of an 86 amu ion fragment at 520 K.

The MVK product showed no secondary consumption by Cl atoms at elevated temperature and no correction was required. This may seem surprising because at ambient temperature and pressure $k(Cl + MVK) = 2 \times 10^{-10}$ cm^3 molecule^{-1} s^{-1}.[23] A rate constant this large would produce large secondary MVK consumption. However, a major reaction channel of this reaction is Cl addition to the double bond, and this addition rate constant

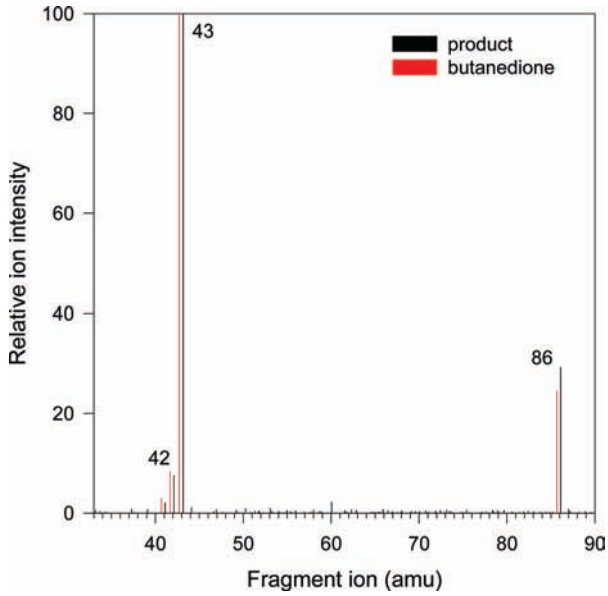

Figure 11. Mass spectrum at 297 K for the product (black bars) observed at the common retention time of MVK and butanedione in the presence of 500 ppm O_2. Red bars represent the mass spectrum of butanedione measured during these experiments.

will decrease as the temperature is increased. One series of experiments was performed to measure this rate constant at 485 K and 700−900 Torr pressure using ethane as the reference species. These experiments yielded a rate constant of 4.5 (±2.5) × 10^{-12} cm^3 $molecule^{-1}$ s^{-1}, a value too small to produce significant secondary consumption of MVK in the butanone experiments at this temperature.

We believe that MVK is formed at high temperature from stabilized 3- and 4-butanonylperoxy radicals by a mechanism similar to formation of C_2H_4 from the $O_2 + C_2H_5$ reaction.[24] Tranter and Walker[25] also observed MVK formation from the reaction of O_2 with 3- and 4-butanonyl radicals at 753 K. The shaded symbols at 490 K were obtained at a total pressure of 150−170 Torr of O_2 with no N_2 added to the initial mixture to test the effect of total pressure on the product yields. There is no significant pressure effect at this temperature for any of the products.

4. Computer Modeling of the Data

The data in Figures 3, 8, 9, and 10 were simulated using the Acuchem chemical kinetics program with the rate constants in Table 2. The rate constants for reactions 1a, 1b, and 1c at 297 K were derived from the yields of 1-chloro-, 3-chloro-, and 4-chlorobutanone in Figure 1 as described in section 3.1.1 with activation energies determined in section 3.2.2. Application of this model to experiments in the absence of added O_2 generated the temperature dependent yield curves of the three chlorobutanones in Figure 8.

No literature values are available for reactions 2 or 3 to our knowledge, but the ratio k_2/k_3 is measured in these experiments at 297 K (see section 3.1.3) for each of the butanonyl radical isomers. As discussed in section 3.1.3, the rate constants for k_{3a}, k_{3b}, and k_{3c} are assumed to be equal to that measured for the reaction of O_2 with the acetonyl (1-methylvinoxy) radical [(1.00 ± 0.25) × 10^{-12} cm^3 $molecule^{-1}$ s^{-1} at ambient temperature and 760 Torr]. Data in Figure 4 of ref 17 indicate that, in the high pressure limit, there is little temperature dependence to the addition reaction of O_2 to the acetonyl radical. Therefore, we have assumed a zero activation energy for reactions 3a, 3b, and 3c. In the absence of data, we have also assumed that reactions 2a, 2b, and 2c have zero activation energies. Measurements have been made of the rate constants of Cl_2 reactions with C_2H_5, *n*- and *iso*-C_3H_7, and *n*- and *t*-C_4H_9,[19,26] as well as $CH_3C(O)$[27] and CH_3OCH_2.[28] For each of these reactions, a small negative activation energy is observed. The fact that these reactions have rate constants ∼100−1000 times greater than those observed for 1- and 3-butanonyl radicals as discussed in section 3.1.3 may indicate that the 1- and 3-butanonyl radical reactions with Cl_2 have a modest positive activation energy. An activation energy of ∼3−4 kcal mol^{-1} would account for the estimated factor of ∼100−1000 slower rate constants at ambient temperature for the 1- and 3-butanonyl + Cl_2 reactions.

No rate data are available for the $RO_2 + R'O_2$ reactions of butanonylperoxy radicals. However, there is a recommended ambient temperature rate constant[29] for the self-reaction of the acetonylperoxy radical ($CH_3C(O)CH_2O_2$) [=8 × 10^{-12} cm^3 $molecule^{-1}$ s^{-1} with an estimated error of a factor of 2]. The rate constants for the peroxy radical reactions in Table 2 have been chosen to be ∼10^{-11}. The specific values for the rate constants were chosen to fit the yields of butanedione and acetaldehyde as functions of temperature in Figure 9 and the butanedione yield as a function of O_2 mole fraction in Figure 3. As an example, the value of k_{6ab} at 297 K was chosen to make the butanedione yield approximate the experimentally observed slow rise after the initial sharp increase presented in Figure 3, while the temperature dependences of k_{5a} and k_{6ab} were chosen to fit the observed decrease in butanedione yield as the temperature increases from 297 to 380 K in Figure 9.

The rate constants of the reverse reactions k_{-3a} and k_{-3c} were initially adjusted to obtain the correct product yields at the temperatures of the midpoints of the rapid increases in the 3- and 1-chlorobutanone mole fractions for the initial conditions of Figure 9 (390 and 425 K, respectively). The absolute values of these rate constants depend on the values chosen for the $RO_2 + R'O_2$ reactions, as discussed below. The activation energy of k_{-3a} was estimated by applying the model to the data in Figure 10, which has an initial O_2 mole fraction 340 times that of Figure 9. Again, the value of k_{-3a} was adjusted until the yield of 3-chlorobutanone at the midpoint of its rise (455 K) is predicted correctly. The values of k_{-3a} at two temperatures yielded an estimated activation energy [$E_a(-3a) = 24.5$ kcal $mole^{-1}$] for reaction −3a. Using this activation energy, and the absolute value of k_{-3a} determined at 390 K, yielded the *A* factor presented in Table 2. The inset in Figure 10 presents the predicted yield of 3-chlorobutanone compared to the experimental data points for two other choices of the activation energy of −3a accompanied by the necessary changes in *A* factor. The activation energy for the solid line (24.5 kcal mol^{-1}) is identical to that in the main figure, while the dotted lines show predictions for a 27 kcal mol^{-1} (upper curve) or 22 kcal mol^{-1} (lower curve) activation energy. These two curves more than span the data scatter.

No evidence of reverse reaction was observed for reaction 3c in Figure 10 at high initial O_2 mole fraction over the temperature range studied. For this reason, it was not possible to estimate the activation energy of the decomposition of 1-chlorobutanonylperoxy radicals back to reactants (reaction −3c) using this method. The activation energy was assumed to be equal to that of 3-chlorobutanonylperoxy (reaction −3a). The value of $A(-3c)$ was calculated from this activation energy and the absolute value of the rate constant required to fit the midpoint in the 1-chlorobutanone rise at 425 K in Figure 9.

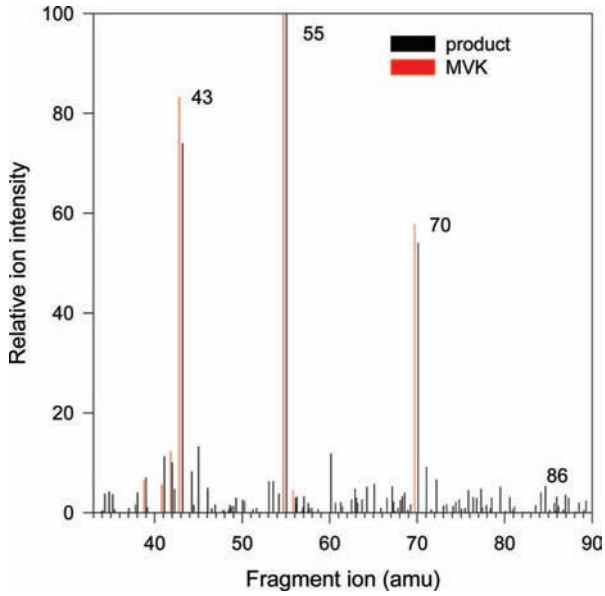

Figure 12. Mass spectrum at 520 K for the product (black bars) observed at the common retention time of MVK and butanedione in the presence of 170 000 ppm O_2. Red bars represent the mass spectrum of methylvinylketone from the NIST/EPA/NIH Mass Spectral Library (2002). The large number of fragment peaks in the experimental spectrum are representative of the ion noise levels.

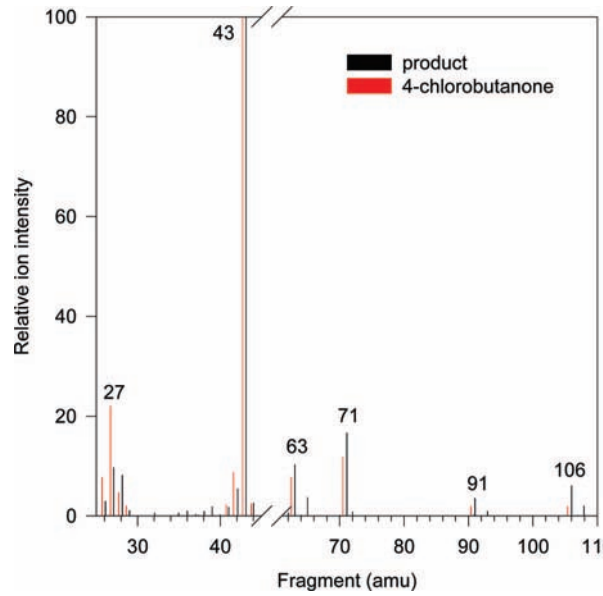

Figure 13. Mass spectrum at 297 K for a primary product (black bars) observed in the absence of added O_2. Red bars represent the mass spectrum of 4-chlorobutanone from the NIST/EPA/NIH Mass Spectral Library (2002).

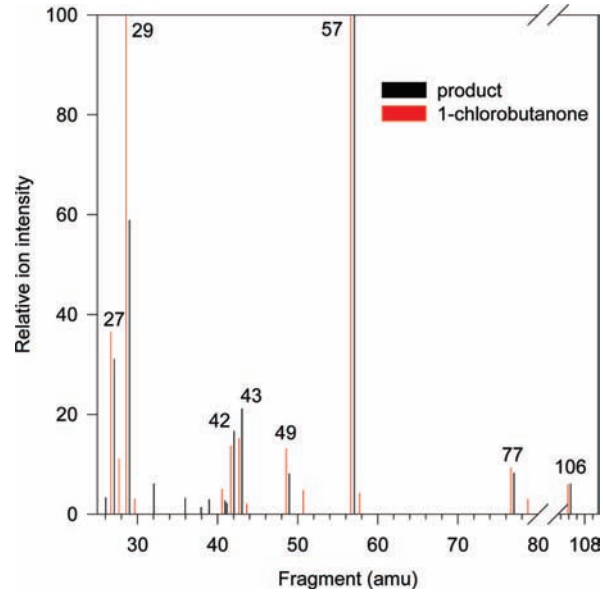

Figure 14. Mass spectrum at 297 K for a primary product (black bars) observed in the absence of added O_2. Red bars represent the mass spectrum of 1-chlorobutanone from the NIST/EPA/NIH Mass Spectral Library (2002).

To test the effect of changes in the values of the peroxy/peroxy radical rate constants on the determination of the activation energy of reaction −3a, the rate constants of all peroxy reactions were decreased by a factor of 100. The absolute rate constant for −3a was decreased by a factor of 10 to again achieve the break in the 3-chlorobutanone yield at the proper temperature in Figure 9. With these new rate constants, the position of the sharp increase in the yield profile of the 3-chlorobutanone in Figure 10 was again predicted correctly using an activation energy of 24.5 kcal. Thus, the position of the increase in Figure 10 depends on the activation energy of reaction −3a, not on the absolute values of the peroxy/peroxy rate constants provided that the A factor of −3a is readjusted to fit the data in Figure 9.

The uncertain activation energy for the reaction of 3-butanonyl radicals with Cl_2 (reaction 2a) does contribute uncertainty to the calculation of $E_a(-3a)$. If the activation energy of reaction 2a is assumed to be 4 kcal mol^{-1} as discussed earlier in this section, the calculated value of $E_a(-3a)$ is reduced to 21.5 kcal mol^{-1}, indicating that assuming a zero activation energy for 2a produces an upper limit to $E_a(-3a)$. On the basis of these chemical simulations and error discussions, we estimate the activation energy of reaction −3a to be 24.5 (+2, −5) kcal mol^{-1}, including data scatter and uncertainty in the activation energy of reaction 2a. Assuming that the activation energy of the O_2 addition reaction 3a is near zero, $E_a(-3a)$ represents the enthalpy of addition of O_2 to the 3-butanonyl radical. The value presented above is consistent with that measured for O_2 addition to acetonyl radicals (−25.1 ± 0.5 kcal mol^{-1}).[17] Recent calculations indicate that there may be a small barrier (2 kcal,[17] 3.5 kcal[16]) to the addition of O_2 to the acetonyl radical, although the calculated magnitudes are in doubt as stated by both authors. Any barrier to reaction 3a will reduce the enthalpy of addition derived from the activation energy of the 3-butanonylperoxy radical decomposition via reaction −3a. Thus, the estimated enthalpy of addition presented above for reaction 3a must be considered to be an upper limit. The actual value could be modestly smaller. This upper limit is much smaller than the enthalpy of addition of O_2 to the ethyl radical which is 34.2−34.5 kcal mol^{-1} (depending on the peroxy conformer) based on ab initio calculation.[30]

Finally, the mechanism of MVK formation at high temperature will be examined by analogy to the mechanism of C_2H_4 formation from the reaction of O_2 with C_2H_5. Experiments[24] and ab initio calculations[30] carried out on the high temperature reaction of the ethyl radical with O_2 have shown that there are two preferred channels for this process. One channel proceeds through a chemically activated ethylperoxy intermediate which decomposes directly to ethylene. The other channel forms ethylene from the stabilized ethylperoxy radical at elevated temperature only. In the case of the ethyl radical, the chemically activated path is pressure dependent and is present at all temperatures studied from ambient to >600 K. The C_2H_4 yield

from the ethyl reaction with O_2 at ambient temperature is inversely dependent on pressure. At high temperature, the reaction path via the stabilized ethylperoxy radical opens and becomes the dominant path. This reaction channel exhibits no pressure dependence.

Similar reaction channels might be expected from the reactions of 3- and 4-butanonyl radicals with O_2. Unfortunately, it is not possible to observe generation of MVK at ambient temperature because the large yield of butanedione at the same GC retention time precludes measurement of a small quantity of MVK. However, at high temperature no butanedione is present to within experimental error and only MVK is observed based on the GC/MS results discussed earlier and presented in the Appendix. The yield of MVK formed from the reaction of O_2 with butanonyl radicals is independent of pressure as shown by the lower pressure data point in Figure 10. This indicates that MVK is formed from a stabilized butanonylperoxy radical at high temperature by analogy to the $O_2 + C_2H_5$ reaction. Because both 3- and 4-butanonylperoxy radicals are present at high temperature under the conditions of Figure 10, it is not possible to determine whether only one or both of these peroxy radicals contribute to the formation of MVK. We have chosen to represent MVK formation solely via the reaction of the 3-butanonylperoxy radical. The rate constant chosen for reaction 11 is obtained by matching the experimental yield of MVK in Figure 10.

$$CH_3C(O)CH(O_2)CH_3 \rightarrow CH_3C(O)CH=CH_2+HO_2 \quad (11)$$

The activation energy for reaction 11 is an estimate based on the calculated barrier to the similar reaction of ethylperoxy radicals, which is 3 kcal below the energy of the reactants for O_2 addition to the ethyl radical.[30] Because our estimated heat of reaction for the addition process of the butanonyl radical (24.5 kcal mol^{-1}) is approximately $^2/_3$ of that for the ethyl reaction with O_2 (34.2 kcal),[30] the activation energy for reaction 11 was estimated to be 2 kcal less than the heat of the addition reaction 3a or 22.5 kcal mol^{-1}.

The lines in Figures 3, 8, 9, and 10 were calculated using the rate constants presented in Table 2. The fits are reasonably good, and the trends are predicted well, indicating that the mechanism in Table 2 captures the main mechanistic features of the reaction of Cl atoms with butanone both in the presence and absence of added O_2. The absolute values of some of the rate constants, however, have substantial uncertainty associated with them as discussed above.

5. Summary and Conclusions

In this experimental study, the rate constants and chemical mechanism of the reaction of Cl atoms with butanone have been examined both in the presence and absence of O_2 as functions of temperature and pressure. The experiments were performed by UV irradiation of Cl_2/butanone/N_2 and Cl_2/butanone O_2/N_2 mixtures. We draw seven major conclusions from these experiments.

First, in the absence of O_2, the only products observed are 1-, 3-, and 4-chlorobutanone with yields of 3.1%, 76%, and 22.5%, respectively, at ambient temperature. On the basis of these yields and the known overall rate constant for Cl reaction with butanone (3.8×10^{-11} cm^3 molecule^{-1} s^{-1}), the rate constants for Cl reaction at each carbon position have been determined at 297 K.

Second, temperature dependent measurements in the absence of O_2 have determined activation energies for H atom abstraction by Cl atoms at the 1-carbon [1800 ($\pm$300) cal mol^{-1}] and 4-carbon [470 ($+$300, $-$150) cal mol^{-1}] positions relative to that of reaction at the 3-position.

Third, addition of O_2 to the reaction mixture at ambient temperature provided measurements of the ratios of the rate constant of the reaction of Cl_2 to that with O_2 for 1-, 3-, and 4-butanonyl [e.g., $CH_3C(O)CH_2CH_2$] radicals. The values of these ratios follow: 0.027, 0.011, and 1.52, respectively. The carbon radical sites next to the carbonyl group (1 and 3 positions) are deactivated with respect to reaction with Cl_2, while the radical at the 4-position maintains a reactivity similar to that typical of alkyl radicals.

Fourth, at ambient temperature, the presence of O_2 reduces the yields of the chlorobutanones and forms oxygenated organic molecules (acetaldehyde, acetyl chloride, butanedione, and propionyl chloride) derived from addition of O_2 to the 1-, 3-, and 4-butanonyl radicals. The sole fate of the 3-butanonoxy radical [$CH_3C(O)CH(O)CH_3$] (formed from $CH_3C(O)CH(O_2)CH_3 + RO_2$ reactions) is decomposition to form CH_3CHO and CH_3CO. Butanedione is formed primarily from the self-reaction of 3-butanonylperoxy radicals [$CH_3C(O)CH(O_2)CH_3$] at O_2 mole fractions $<$500 ppm. As the O_2 mole fraction is increased from 500 to 1100 ppm, additional butanedione is produced by the reaction of 3-butanonylperoxy with 4-butanonylperoxy radicals. Propionyl chloride is formed from decomposition of the 1-butanonoxy radical.

Fifth, increasing the temperature to $\sim$400 K causes the O_2 addition reaction to the 1- and 3-butanonyl radicals to reverse at moderate O_2 concentrations. This reversal suppresses the formation of oxygenated species with accompanying increases in the chlorobutanone yields until they reach levels similar to those in the absence of O_2 at ambient temperature. Varying the O_2 concentration at high temperature provides an estimate of the exothermicity of the addition of O_2 to the 3-butanonyl radical ($=$24.5 kcal mol^{-1}).

Sixth, at temperatures of $\sim$490 K in the presence of air, a new channel opens which forms methylvinylketone via decomposition of 3- and/or 4-butanonylperoxy radicals.

Seventh, the overall rate constant for the reaction of Cl with butanone (reaction 1) was measured over the range 297 $-$ 475 K. No discernible temperature dependence is observed [$E_a(1) = 0 \pm 200$ cal mol^{-1}].

Appendix: GC/MS Spectra

A GC/MS instrument was used to identify specific chemical species of importance to these experiments. As discussed in the main text, two of these species (butanedione and methylvinylketone) coeluted from the GC column at exactly the same retention time. Figure 11 presents the GC/MS spectrum of the product (black lines) at this retention time after irradiation at 297 K in the presence of 500 ppm O_2. A spectrum of butanedione was also run on this instrument, which is shown as red lines in this figure. The largest ion fragments present are the molecular ion of butanedione at 86 amu and the major fragment (CH_3CO^+) at 43 amu. The nearly perfect match identifies butanedione as the product present at this retention time under these conditions.

At 520 K and 170 000 ppm of O_2, irradiation produced a very different product spectrum at this retention time as shown in Figure 12. The many small ion peaks in the product spectrum are representative of the higher noise level in these high temperature experiments. No 86 amu ion is observed under these conditions at the coeluting retention time above the noise level. Instead a spectrum is observed which matches that of meth-

ylvinylketone. In this case, the MVK standard spectrum is obtained from the NIST/EPA/NIH Mass Spectral Library (2002). The principal ion fragments from MVK are the following: the molecular mass at 70 amu, CH_2CHCO^+ at 55 amu, and CH_3CO^+ at 43 amu.

Neither 1- nor 4-chlorobutanone was available commercially for use in determining the retention times of these species on the GC column. For that reason, samples from selected irradiated mixtures at 297 K in the absence of added O_2 were analyzed on both the GC/FID and GC/MS instruments. This allowed determination of the identity of two unknown chromatographic peaks present in the GC/FID analysis using the GC/MS data presented in Figures 13 and 14. The GC product peak which produced the mass spectrum in Figure 13 was identified as 4-chlorobutanone on the basis of the standard spectrum from the NIST/EPA/NIH Mass Spectral Library (2002). The major fragments are the following: the molecular mass at 106 amu, $CH_2ClCH_2CO^+$ at 91 amu, $CH_3COCH_2CH_2^+$ at 71 amu, $CH_2CH_2Cl^+$ at 63 amu, and CH_3CO^+ at 43 amu. The product whose mass spectrum is shown Figure 14 is identified as 1-chlorobutanone on the basis of the standard spectrum again taken from the NIST 2002 Database. For this species, selected major ion fragments are the following: molecular mass at 106 amu, CH_2ClCO^+ at 77 amu, $CH_3CH_2CO^+$ at 57 amu, CH_2Cl at 49 amu, and $CH_3CH_2^+$ at 29 amu.

Acknowledgment. We acknowledge critical assistance provided by Professor Craig Donahue at the University of Michigan—Dearborn. We also acknowledge the support of Professor Ali Bazzi at UM—D, who provided access to the GC/MS used during these experiments.

References and Notes

(1) Kaiser, E. W.; Wallington, T. J. *J. Phys. Chem. A* **2007**, *111*, 10667–10670.
(2) Iwasaki, E.; Taketani, F.; Takahashi, K.; Matsumi, Y.; Wallington, T. J.; Hurley, M. D. *Chem. Phys. Lett.* **2007**, *439*, 274–279.
(3) Kaiser, E. W.; Donahue, C. J.; Pala, I. R.; Wallington, T. J.; Hurley, M. D. *J. Phys. Chem. A.* **2007**, *111*, 1286–1299.
(4) Bryukov, M. G.; Slagle, I. R.; Knyazev, V. D. *J. Phys. Chem. A* **2002**, *106*, 10532–10542.
(5) Braun, W.; Herron, J. T.; Kahaner, D. K. *Int. J. Chem. Kinet.* **1988** **20**, 51.
(6) Tyndall, G. S.; Orlando, J. J.; Kegley-Owen, C. S.; Wallington, T. J.; Hurley, M. D. *Int. J. Chem. Kinet.* **1999**, *31*, 776–784.
(7) Carr, S.; Shallcross, D. E.; Canosa-Mas, C. E.; Wegner, J. C.; Sidebottom, H. W.; Treacy, J. J.; Wayne, R. P. *Phys. Chem. Chem. Phys.* **2003**, *5*, 3874–3883.
(8) Shi, J.; Wallington, T. J.; Kaiser, E. W. *J. Phys. Chem.* **1993**, *97*, 6184–6192.
(9) Atkinson, R.; Baulch, D. L.; Cox, R. A.; Crowley, J. N.; Hampson, R. F., Jr.; Jenkin, M. E.; Kerr, J. A.; Rossi, M. J.; Troe, J. IUPAC Subcommittee on Gas Kinetic Data Evaluation, http:// www.iupac-kinetic.ch.cam.ac.uk/index.html (June 2006).
(10) Tyndall, G. S.; Orlando, J. J.; Wallington, T. J.; Dill, M.; Kaiser, E. W. *Int. J. Chem. Kinet.* **1997**, *29*, 43–55.
(11) Christensen, L. K.; Sehested, J.; Nielsen, O. J.; Wallington, T. J.; Guschin, A.; Hurley, M. D. *J. Phys. Chem. A* **1998**, *102*, 8913–8923.
(12) Taatjes, C. A.; Christensen, L. K.; Hurley, M. D.; Wallington, T. J. *J. Phys. Chem. A* **1999**, *103*, 9805–9814.
(13) Orlando, J. J.; Tyndall, G. S.; Vereecken, L.; Peeters, J. *J. Phys. Chem. A* **2000**, *104*, 11578–11588.
(14) Kaiser, E. W. *J. Phys. Chem.* **1993**, *97*, 11681–11688.
(15) Kaiser, E. W.; Wallington, T. J.; Andino, J. M. *Chem. Phys. Lett.* **1990**, *168*, 309–313.
(16) Kovacs, G.; Zador, J.; Farkas, E.; Nadasdi, R.; Szilagyi, I.; Dobe, S.; Berces, T.; Marta, F.; Lendvay, G. *Phys. Chem. Chem. Phys.* **2007**, *9*, 4142–4154.
(17) Hassouna, M.; Delbos, E.; Devolder, P.; Viskolcz, B.; Fittschen, C. *J. Phys. Chem.A* **2006**, *110*, 6667–6672.
(18) Oguchi, T.; Miyoshi, A.; Koshi, M.; Matsui, H.; Washida, N. *J. Phys. Chem.A* **2001**, *105*, 378–382.
(19) Timonen, R. S.; Gutman, D. *J. Phys. Chem.* **1986**, *90*, 2987–2991.
(20) Bryukov, M. G.; Slagle, I. R.; Knyazev, V. D. *J. Phys. Chem. A* **2003**, *107*, 6565–6573.
(21) Zhao, Z.; Huskey, D. T.; Nicovich, J. M.; Wine, P. H. *Int. J. Chem. Kinet.* **2008**, *40*, 259–267.
(22) Cuevas, C. A.; Notario, A.; Martinez, E.; Albaladejo, J. *Phys. Chem. Chem. Phys.* **2004**, *6*, 2230–2236.
(23) Orlando, J. J.; Tyndall, G. S.; Apel, E. C.; Riemer, D. D.; Paulson, S. E. *Int. J. Chem. Kinet* **2003**, *35*, 334–353.
(24) Kaiser, E. W. *J. Phys. Chem.A* **2002**, *106*, 1256–1265.
(25) Tranter, R. S.; Walker, R. W. *Phys. Chem. Chem. Phys.* **2001**, *3*, 1262–1270.
(26) Eskola, A. J.; Lozovsky, V. A.; Timonen, R. S. *Int. J. Chem. Kinet.* **2007**, *39*, 614–619.
(27) Maricq, M. M.; Szente, J. J. *Chem. Phys. Lett.* **1996**, *253*, 333–339.
(28) Maricq, M. M.; Szente, J. J.; Hybl, J. D. *J. Phys. Chem. A* **1997**, *101*, 5155–5167.
(29) Atkinson, R.; Baulch, D. L.; Cox, R. A.; Crowley, J. N.; Hampson, R. F.; Hynes, R. G.; Jenkin, M. E.; Rossi, M. J.; Troe, J. *Atmos. Chem. Phys.* **2006**, *6*, 3625–4055.
(30) Wilke, J. J.; Allen, W. D.; Schaefer, H. F., III. *J. Chem. Phys.* **2008**, *128*, 74308.

JP809169H